Color distribution from multicolor LED arrays

Ivan Moreno, Ulises Contreras

Unidad Academica de Fisica, Universidad Autonoma de Zacatecas, Zacatecas 98060, Mexico
imoreno@planck.reduaz.mx

Abstract: We describe a fully-analytical, simple yet sufficiently accurate method to compute the color pattern of the light emitted from multicolor light-emitting diode (LED) assemblies. Spatial distributions for both color variation and correlated color temperature (CCT) as a function of typical parameters of influence, such as LED spectrum, spatial distribution of LED radiation, target distance, LED-to-LED spacing, and number of LEDs, are shown. To illustrate the method, we simulate and analyze the color patterns of linear, ring, and square RGB (red, green, and blue) arrays for Lambertian-type, batwing, and side emitting LEDs. Our theory may be useful to choose the optimal value for both the array configuration and the array-diffuser distance for lighting systems with color mixing devices.

OCIS codes: (330.1690) Color; (230.3670) Light emitting diodes; (220.4830) Optical system design.

References and links

1. A. Zukauskas, M. S. Schur, R. Gaska, *Introduction to Solid State Lighting* (Wiley-Interscience, New York, 2002).
2. I. Ashdown, "Solid-state lighting design requires a system-level approach," SPIE Newsroom (2006). http://newsroom.spie.org/x2235.xml?highlight=x531
3. D. Malacara, *Color Vision and Colorimetry*, SPIE Press, Bellingham WA, USA, 2002.
4. G. Wyszecki, and W. S. Styles, *Color Science: Concepts and Methods, Quantitative Data and Formulae* (2nd ed.), (Wiley, New York, 1982).
5. Y. Ohno, "Radiometry and Photometry Review for Vision Optics," *in Handbook of Optics* (Vol. III, 2nd ed.), M. Bass, J. M. Enoch, E. W. Van Stryland, W. L. Wolfe, Eds (McGraw-Hill, 2001).
6. M. Strojnik, G. Paez, "Radiometry," *in Handbook of Optical Engineering*, D. Malacara, B. Thompson, Eds. (2001).
7. Y. Uchida, T. Taguchi, "Lighting theory and luminous characteristics of white light-emitting diodes," Opt. Eng. **44**, 124003–1 (2005).
8. Y. Gu, N. Narendran, T. Dong, H. Wu, "Spectral and luminous efficacy change of high-power LEDs under different dimming methods," in *Sixth International Conference on Solid State Lighting*, I. T. Ferguson, N. Narendran, T. Taguchi, I. E. Ashdown, eds., Proc. SPIE **6337**, 63370J:1-7 (2006).
9. Y. Ohno, "Spectral design considerations for white LED color rendering," Opt. Eng. **44**, 111302-1 (2005).
10. H. Y. Chou, T. H. Hsu, T. H. Yang, "Effective method for improving illuminating properties of white-light LEDs," in *Light-Emitting Diodes: Research, Manufacturing, and Applications IX*; Steve A. Stockman, H. Walter Yao, E. Fred Schubert; Eds., Proc. SPIE **5739**, p. 33-41 (2005).
11. H. Ries, I, Leike, J. Muschaweck, "Optimized additive mixing of colored light-emitting diode sources," Opt. Eng. **43**, 1531-1356 (2004).
12. A. Zukauskas, R. Vaicekauskas, F. Ivanauskas, R Gaska, M. S. Shur, "Optimization of white polychromatic semiconductor lamps," Appl. Phys. Lett. **80**, 234-236 (2002).
13. E. F. Schubert, *Light-emitting diodes* (Cambridge University Press, Cambridge, 2003).
14. I. Moreno, M. Avendaño-Alejo, R. I. Tzonchev, "Designing light-emitting diode arrays for uniform near-field irradiance," Appl. Opt. **45**, 2265-2272 (2006).
15. I. Moreno, J. Muñoz, R. Ivanov, "Uniform illumination of distant targets using a spherical LED array," Opt. Eng. **46** (3), (In press 2007).
16. Y. Uchida, T. Taguchi, "Lighting theory and luminous characteristics of white light-emitting diodes," Opt. Eng. **44**, 124003–1 (2005).
17. I. Moreno, "Spatial distribution of LED radiation," in *The International Optical Design Conference*, G. Gregory, J. Howard, J. Koshel, eds., Proc. SPIE **6342**, 634216:1-7 (2006).
18. I. Moreno, "Simple functions for intensity and irradiance distribution from LEDs," in preparation.

#78265 - $15.00 USD Received 19 December 2006; revised 27 February 2007; accepted 28 February 2007

19. I. Ashdown, "Chromaticity and color temperature for architectural lighting," in *Solid State Lighting II*, I. T. Ferguson, N. Narendran, S. P. DenBaars, Y. S. Park, eds., Proc. SPIE **4776**, 51-60 (2002).
20. J. Hernández-Andrés, R. L. Lee, Jr., J. Romero, "Calculating correlated color temperatures across the entire gamut of daylight and skylight chromaticities," Appl. Opt. **38**, 5703-5709 (1999).
21. C. S. McCamy, "Correlated color temperature as an explicit function of chromaticity coordinates," Color Res. Appl. **17**, 142-144 (1992).
22. J. M. Gaines, "Modelling of multichip LED packages for illumination," Light. Res. Technol. **38**, 153-165 (2006).
23. I. Moreno, L. M. Molinar, "Color uniformity of the light distribution from several cluster configurations of multicolor LEDs." in *Fifth International Conference on Solid State Lighting*, I. T. Ferguson, J. C. Carrano, T. Taguchi, I. E. Ashdown, eds., Proc. SPIE **5941**, 359-365 (2005).

1. Introduction

Solid-state lighting (SSL) is a rapidly emerging field that is mainly based on light-emitting diodes (LEDs) [1]. This technology has surpassed the characteristics of incandescent lamps in luminous efficiency, durability, reliability, safety, and power requirements. Though modern high power LEDs are highly efficient devices, several LEDs must be mounted on panels to obtain practical luminous fluxes. LEDs assembling an array can be chosen to emit light in a wide variety of highly saturated colors. As a consequence, a source made of multicolor LEDs easily allows the user to dynamically select the desired color point of the lamp without additional filters. In addition to this color adjustability, for some applications LED arrays can be designed to produce emissions into different color patterns. However, for most applications a uniform color distribution is desired. The output color distribution from multicolor LED arrays shows distinctive patterns with color separation, which is a function of several parameters such as array configuration and panel-target distance. Analysis of color distribution is an important issue that must be addressed in SSL design [2].

In what follows, we describe in detail our generalized method for computing the color distribution of the light from multicolor LED assemblies (Sec. 2). In Sec. 3 we illustrate the method being applied for typical sample arrays. An experimental example is shown in Sec. 4, and our conclusions are summarized in Sec. 5.

2. Color distribution

The output color distribution from a multicolor LED array shows distinctive patterns with clear color separation, in particular, when the extended nature of the source is evident because the target distance is not large enough. At these distances radiant intensity can be difficult to interpret because a LED array is a quite extended source, and computation of angular distribution of color may not be appropriate. Therefore, we consider irradiance distribution to analyze the color distribution over a flat area parallel to the surface of the LED array.

We first review and express additive color mixing as linear equations in function of relative irradiance ratios (Sec. 2.1), and then determine the relative irradiances necessary to achieve a desired color (Sec. 2.2). Simple yet practical analytical irradiance distributions (Sec. 2.3) are described for computation of the color pattern from multicolor LED arrays (Sec. 2.4). Color uniformity of the light distribution is discussed in Sec. 2.5.

2.1 Color mixing

The chromaticity coordinates (in the CIE 1931 diagram) of a light source with LEDs of *S* different colors are given by [3]:

$$x_T = \frac{\sum_{i=1}^{S} X_i}{\sum_{i=1}^{S} (X_i + Y_i + Z_i)}, \qquad y_T = \frac{\sum_{i=1}^{S} Y_i}{\sum_{i=1}^{S} (X_i + Y_i + Z_i)}, \qquad z_T = 1 - x_T - y_T \ . \tag{1}$$

#78265 - $15.00 USD Received 19 December 2006; revised 27 February 2007; accepted 28 February 2007

Here, X_i, Y_i, and Z_i are the tristimulus values for the ith color [3,4]:

$$X_i = k\int_{400nm}^{700nm} E_i(\lambda)\bar{x}(\lambda)\mathrm{d}\lambda\,,\quad Y_i = k\int_{400nm}^{700nm} E_i(\lambda)\bar{y}(\lambda)\mathrm{d}\lambda,\qquad Z_i = k\int_{400nm}^{700nm} E_i(\lambda)\bar{z}(\lambda)\mathrm{d}\lambda\,, \tag{2}$$

where k is a proportionality constant that relates spectral radiance [3] or spectral radiant power [4], with spectral irradiance $E_i(\lambda)$ [5,6]. The color-matching functions are denoted by $\bar{x}(\lambda)$, $\bar{y}(\lambda)$, and $\bar{z}(\lambda)$. Equation (2) can be expressed in terms of the unitary spectral irradiance $U_i(\lambda)=E_i(\lambda)/E_{\text{peak-}i}$, where $E_{\text{peak-}i} = E_i(\lambda_{\text{peak}})$, to provide tristimulus expressions that linearly depend on peak irradiance:

$$X_i = kE_{peak\text{-}i}\int_{400nm}^{700nm} U_i(\lambda)\bar{x}(\lambda)\mathrm{d}\lambda = kE_{peak\text{-}i}\hat{X}_i\,,\qquad Y_i = kE_{peak\text{-}i}\int_{400nm}^{700nm} U_i(\lambda)\bar{y}(\lambda)\mathrm{d}\lambda = kE_{peak\text{-}i}\hat{Y}_i\,,$$

$$Z_i = kE_{peak\text{-}i}\int_{400nm}^{700nm} U_i(\lambda)\bar{z}(\lambda)\mathrm{d}\lambda = kE_{peak\text{-}i}\hat{Z}_i\,. \tag{3}$$

Here $\hat{X}_i$, $\hat{Y}_i$, and $\hat{Z}_i$ are the normalized tristimulus values for the ith color, which for practical purposes remain almost constant when the emitted power changes. This approximation is valid for LEDs because peak wavelength and spectral width do not change considerably when adjusting the drive current [7,8]. However, if the output color is dynamically varied over a wide range, the peak wavelength shift [<3nm (blue and white LED), <8nm (red LED), <12 nm (green LED)], due to drive current change, must be included in Eq.(3) [7,8]. Therefore, if color is tuned over a wide range of color temperatures, it can be more appropriate to drive blue LEDs because, in addition to the short wavelength shift, blue light contributes less to the luminance [3,4]. A simple yet sufficiently accurate mathematical model for the relative spectrum $U_i(\lambda)$ of an LED is given by [9]:

$$U_i(\lambda) = \tfrac{1}{3}\left[g_i(\lambda) + 2g_i^5(\lambda)\right], \tag{4}$$

where $g_i(\lambda)=\exp\{-[(\lambda-\lambda_i)/\Delta\lambda_i]^2\}$, λ_i is the peak wavelength and $\Delta\lambda_i$ is the half spectral width. An LED lamp can also combine phosphor-type white LEDs with colored LEDs [10]. In this case, the simulation of the white spectrum is quite different [9].

Therefore, from Eq. (3) the chromaticity coordinates of Eq. (1) can be expressed as:

$$x_T = \frac{\sum_{i=1}^{S} e_{i1}\hat{X}_i}{\sum_{i=1}^{S} e_{i1}\left(\hat{X}_i+\hat{Y}_i+\hat{Z}_i\right)}\,,\qquad y_T = \frac{\sum_{i=1}^{S} e_{i1}\hat{Y}_i}{\sum_{i=1}^{S} e_{i1}\left(\hat{X}_i+\hat{Y}_i+\hat{Z}_i\right)}\,,\qquad z_T = 1-x_T-y_T\,. \tag{5}$$

where $e_{i1}=E_{\text{peak-}i}/E_{\text{peak-1}}$ are the relative peak irradiances for each color. Depending on the application, e_{i1} can also be taken as relative radiant flux or as relative peak intensity [3-6].

2.2 Relative peak irradiance for color mixing

The relative peak irradiances necessary to achieve a desired color with chromatic coordinates (x_T, y_T, z_T,) can determined by solving three linear Eqs.:

$$\sum_{i=1}^{S} e_{i1}\left[\left(1-x_T^{-1}\right)\hat{X}_i+\hat{Y}_i+\hat{Z}_i\right]=0\,,\quad \sum_{i=1}^{S} e_{i1}\left[\hat{X}_i+\left(1-y_T^{-1}\right)\hat{Y}_i+\hat{Z}_i\right]=0\,,\quad \sum_{i=1}^{S} e_{i1}\left[\hat{X}_i+\hat{Y}_i+\left(1-z_T^{-1}\right)\hat{Z}_i\right]=0\,. \tag{6}$$

If more than four sources of different colors are mixed, the relative peak irradiances necessary to achieve the desired color are no longer unique. For S LEDs of different colors there are S-3 degrees of freedom to mix a given color [11].

The most popular multicolor source is the RGB. For a RGB-LED array S=3, and relative peak irradiances are given by:

#78265 - $15.00 USD Received 19 December 2006; revised 27 February 2007; accepted 28 February 2007

$$e_{G-R}=\frac{x_T\left(\hat{Y}_R\hat{Z}_B-\hat{Y}_B\hat{Z}_R\right)+y_T\left(\hat{X}_B\hat{Z}_R-\hat{X}_R\hat{Z}_B\right)+z_T\left(\hat{X}_R\hat{Y}_B-\hat{X}_B\hat{Y}_R\right)}{x_T\left(\hat{Y}_B\hat{Z}_G-\hat{Y}_G\hat{Z}_B\right)+y_T\left(\hat{X}_G\hat{Z}_B-\hat{X}_B\hat{Z}_G\right)+z_T\left(\hat{X}_B\hat{Y}_G-\hat{X}_G\hat{Y}_B\right)},$$

$$e_{B-R}=\frac{x_T\left(\hat{Y}_G\hat{Z}_R-\hat{Y}_R\hat{Z}_G\right)+y_T\left(\hat{X}_R\hat{Z}_G-\hat{X}_G\hat{Z}_R\right)+z_T\left(\hat{X}_G\hat{Y}_R-\hat{X}_R\hat{Y}_G\right)}{x_T\left(\hat{Y}_B\hat{Z}_G-\hat{Y}_G\hat{Z}_B\right)+y_T\left(\hat{X}_G\hat{Z}_B-\hat{X}_B\hat{Z}_G\right)+z_T\left(\hat{X}_B\hat{Y}_G-\hat{X}_G\hat{Y}_B\right)}. \quad (7)$$

For some applications, these ratios may be selected to maximize several lighting parameters of importance such as efficacy and color rendering index [11,12].

If the spectral linewidth of colored LEDs is quite narrow, then the normalized tristimulus values may be approximated by the corresponding color-matching functions [13], i. e. $\hat{X}\approx\bar{x}(\lambda_{peak})$, $\hat{Y}\approx\bar{y}(\lambda_{peak})$, and $\hat{Z}\approx\bar{z}(\lambda_{peak})$. This can be useful to give a quick approximation from most manufacturer datasheets. However, if an accurate simulation is required, we recommend using the complete spectrum (which is sometimes supplied by the manufacturer but most of the time must be measured in the laboratory).

2.3 Irradiance distribution

In the following, when we speak of irradiance, we refer to the peak value of spectral irradiance. Because we assume that the illuminated object is a flat surface, we write the irradiance (Wm^{-2}) pattern for an LED displaced to position (x_i,y_i,z_i) over the array surface in terms of Cartesian coordinates (x,y,z). We compute irradiance with arbitrary units because the absolute value of irradiance is not necessary to compute color variations in the CIE *xy* diagram.

The previous Eqs. can be applied to any number of colors; however, for simplicity, we will only analyze typical RGB arrays. For a RGB-LED assembly (see Fig. 1), the relative irradiance distribution of each color with respect to the irradiance distribution of red LEDs, for an array with N_R+N_G+N_B LEDs, is given by:

$$\varepsilon_{G,B\text{-}R}(x,y,z)=e_{G,B\text{-}R}\left[\frac{\sum_i^{N_{G,B}}E_{G,B}(x,y,z;x_i,y_i)}{\sum_i^{N_{G,B}}E_{G,B}(0,0,z_0;x_i,y_i)}\right]\left[\frac{\sum_i^{N_R}E_R(x,y,z;x_i,y_i)}{\sum_i^{N_R}E_R(0,0,z_0;x_i,y_i)}\right]^{-1}, \quad (8)$$

where $E_{R,G,B}(x,y,z;x_i,y_i)$ is the irradiance distribution of each single LED, where $(E_R)_{max}$=$(E_G)_{max}$=$(E_B)_{max}$. Values $e_{G\text{-}R}$ and $e_{B\text{-}R}$ are the relative irradiances of the green and blue LED arrays in relation to the red array, which are necessary to produce the design color in the center (0,0,z_0) of the illuminated region. The $e_{G\text{-}R}$ and $e_{B\text{-}R}$ values are calculated from Eq. (7) according to the selected value of chromatic coordinates (x_T, y_T, z_T) in the pattern center at a distance z_0 from the array. A simple modification of Eq. (8) permits the analysis of assemblies with more than three colors.

Traditionally, a single LED is optically modeled on realistic numerical models based on ray tracing. Because of the time required to trace millions of rays, we recommend that these models be used at the final stage of LED array design. Analytical models are required to practically and quickly analyze multicolor LED arrays. The radiant intensity distribution (Wsr^{-1}) of Lambertian-type LEDs (e.g., some Nichia, Cree, Philips Lumileds, Toyoda Gosei and Osram LEDs) can be modeled as a simple power law of the viewing-angle cosine function [14-16]. Analytic derivation of the LED intensity distribution [17] indicates that complex radiation patterns like that of batwing distributions can be analytically modeled considering the contributions of chip surfaces and reflecting cup in a practical way [18].

The irradiance pattern (normalized to z=1) for a Lambertian-type LED displaced to position (x_i,y_i) over the array surface in terms of Cartesian coordinates (x,y,z) may be expressed as [14,16,18]:

#78265 - $15.00 USD Received 19 December 2006; revised 27 February 2007; accepted 28 February 2007

$$E(x,y,z;x_i,y_i)=\frac{z^{m+1}}{\left[(x-x_i)^2+(y-y_i)^2+z^2\right]^{\frac{m+3}{2}}} \quad . \tag{10}$$

The number m is given by the angle $\theta = \theta_{½}$. This value is typically provided by the manufacturer, defined as the view angle when radiant intensity (normalized intensity is simply $\cos^m\theta$) is half of the value at 0°, i.e. $m=-\ln 2/\ln(\cos\theta_{½})$. m depends on the relative position of the LED emitting region from the curvature center of the spherical encapsulant [17]. If the chip position coincides with the curvature center, the number m is nearly 1 (i.e., $\theta_{½}\approx 60^{\circ}$), and the source is nearly a perfect Lambertian. Usual LEDs are often highly directional emitters, and m is large (e.g., some Nichia® LEDs).

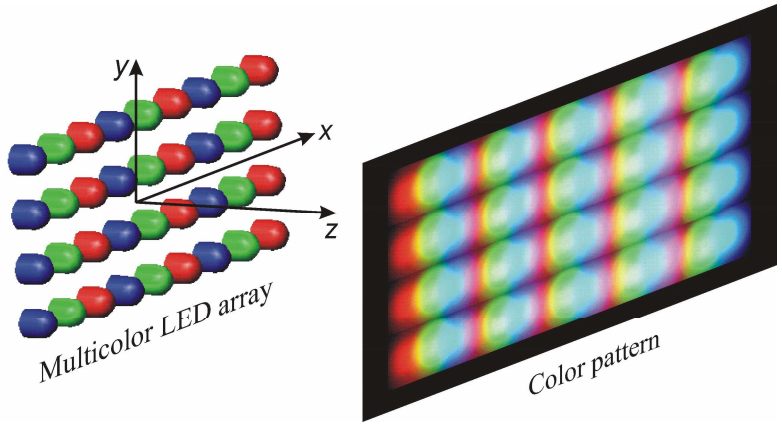

Fig. 1 Multicolor LED assembly that produces a color distribution over a flat surface located in front.

For a batwing radiation pattern, relative irradiance (over every point (x,y) on a flat screen at distance z) from an LED displaced to position (x_i,y_i) over the array surface may be expressed as [18]:

$$E(x,y,z;x_i,y_i)=\frac{Cz^3}{\left[(x-x_i)^2+(y-y_i)^2+z^2\right]^{\frac{5}{2}}}+\frac{z\left[z\cos\alpha+\sqrt{(x-x_i)^2+(y-y_i)^2}\sin\alpha\right]^n}{\left[(x-x_i)^2+(y-y_i)^2+z^2\right]^{\frac{n+3}{2}}} \quad . \tag{11}$$

Here n determines batwing width, α specifies wing angle, and C is a constant that determines the relative irradiance value on the center of the pattern. For example, the typical batwing representative spatial radiation pattern of Luxon® emitters of Philips Lumileds Lighting can be reproduced with n=35, C=1.0, and α=35º (for Red LXHL−BD01, Green, Cyan, Blue and Royal Blue).

Another popular type of radiation pattern is that one of a side emitting LED. These LEDs have the ability to illuminate a large surface located at near distance. The relative irradiance on a flat screen, from a side emitting LED displaced on the array, is [18]:

$$E(x,y,z;x_i,y_i)=\sum_{i=1}^{5}\frac{C_j z\left[z\cos\alpha+\sqrt{(x-x_i)^2+(y-y_i)^2}\sin\alpha\right]^{Mi}}{\left[(x-x_i)^2+(y-y_i)^2+z^2\right]^{\frac{Mi+3}{2}}} \quad . \tag{12}$$

A Luxon® side emitter can be reproduced with: C_1=0.23, C_2=0.3, C_3=1.0, C_4=0.65, C_5=0.15; M_1=200, M_2=45, M_3=40, M_4=7, M_5=80; and α_1=0º, α_2=15º, α_3=85º, α_4=80º, α_5=35º.

In addition, for reference, some radiant intensity distributions retrieved from the previous irradiance Eqs. are shown in Fig. 2.

#78265 - $15.00 USD Received 19 December 2006; revised 27 February 2007; accepted 28 February 2007

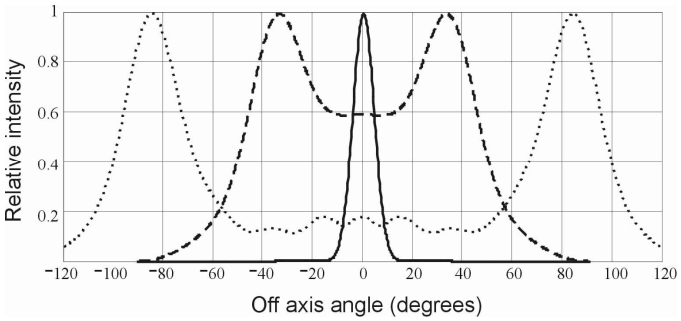

Fig. 2. Examples of simulated LED intensity distribution obtained from analytical irradiance functions, Eqs. (10)-(12). ─Lambertian type emitter with $\theta_{½}$ =5°, - - - Luxon® batwing emitter, and ····Luxon® side emitter.

2.4 Color distribution

Color spatial pattern of the light from multicolor LED assemblies is determined by the distribution of chromaticity coordinates (x_d,y_d) over the illuminated region. The color distribution for a RGB-LED array can then be calculated from Eq. (5) by

$$x_d(x,y,z)=\frac{\hat{X}_R+\hat{X}_G\varepsilon_{GR}(x,y,z)+\hat{X}_B\varepsilon_{BR}(x,y,z)}{\left(\hat{X}_R+\hat{Y}_R+\hat{Z}_R\right)+\left(\hat{X}_G+\hat{Y}_G+\hat{Z}_G\right)\varepsilon_{GR}(x,y,z)+\left(\hat{X}_B+\hat{Y}_B+\hat{Z}_B\right)\varepsilon_{BR}(x,y,z)},$$

$$y_d(x,y,z)=\frac{\hat{Y}_R+\hat{Y}_G\varepsilon_{GR}(x,y,z)+\hat{Y}_B\varepsilon_{BR}(x,y,z)}{\left(\hat{X}_R+\hat{Y}_R+\hat{Z}_R\right)+\left(\hat{X}_G+\hat{Y}_G+\hat{Z}_G\right)\varepsilon_{GR}(x,y,z)+\left(\hat{X}_B+\hat{Y}_B+\hat{Z}_B\right)\varepsilon_{BR}(x,y,z)}, \quad (13)$$

where ε_{GR} and ε_{BR} are given by Eq. (8).

Usually the color uniformity is analyzed by means of correlated color temperature (CCT) [19]. There are several numerical methods for calculating CCT [4]. Recently, two new simple Eqs. to compute CCT from CIE 1931 *xy* chromaticity coordinates have been developed [20,21]. Because there is a broad CCT range for light from multicolor LED arrays, for CCT>4000 K we recommend using [20]:

$$CCT(x,y,z)=A_0+\sum_{i=1}^{3}A_i\exp\left[-n(x,y,z)/t_i\right], \quad (14)$$

where the value of parameters depend on the CCT range. For a CCT range of 3000−50,000K: A_0=-949.86315, A_1=6253.80338, A_2=28.70599, A_3=0.00004, t_1=0.92159, t_2=0.20039, and t_3=0.07125. A range of CCT=50,000−800,000K requires: A_0=-36284.48953, A_1=0.00228, A_2=5.4535E-36, A_3=0, t_1=0.92159, t_2=0.20039, and t_3=0.

For CCT<4000 K, we suggest the function [21]:

$$CCT(x,y,z)=a\,n^3(x,y,z)+b\,n^2(x,y,z)+c\,n(x,y,z)+d, \quad (15)$$

where a=−449, b=3525, c= −6823.3 and d=5520.33. Parameter n is given by:

$$n(x,y,z)=\frac{x_d(x,y,z)-x_e}{y_d(x,y,z)-y_e}. \quad (16)$$

Here x_d and y_d are given by Eq. (13). The CCT epicenter is located at x_e and y_e. For Eq. (14): x_e=0.3366, and y_e=0.1735 (over the range 3000−50,000K); x_e=0.3356 and y_e=0.1691 for CCT=50000−800,000K. In Eq. (15), epicenter values are x_e=0.3320 and y_e=0.1858.

#78265 - $15.00 USD Received 19 December 2006; revised 27 February 2007; accepted 28 February 2007

2.5. Color uniformity

The lighting industry usually quantifies the color variation of a light source based on the distance (in a uniform color space) of the lamp from a reference color point. Thus, a homogeneous color illumination has a color variation value of zero over the illuminated area. To quantify the non-homogeneity of color, the color error distribution $\Delta uv(x,y,z)$ over a target plane (screen at z position) can be used, which is given by

$$\Delta uv(x,y,z)=\sqrt{[u'(x,y,z)-u'(0,0,z)]^2+[v'(x,y,z)-v'(0,0,z)]^2}\,, \tag{17}$$

where $[u'(x,y,z),\ v'(x,y,z)]$ are the color coordinates of the light source in the CIE 1976 uniform color system:

$$u'(x,y,z)=\frac{4x_d(x,y,z)}{-2x_d(x,y,z)+12y_d(x,y,z)+3},\quad v'(x,y,z)=\frac{9y_d(x,y,z)}{-2x_d(x,y,z)+12y_d(x,y,z)+3}, \tag{18}$$

where x_d and y_d are given by Eq. (13). As a reference, $[u'(0,0,z),\ v'(0,0,z)]$ are the color coordinates on the center of the pattern at distance z.

To quantify the color uniformity of a light source over an illuminated surface, $\Delta uv(x,y)$ is commonly plotted. One is usually interested in determining a single value, i.e. a merit function, which is related to the color uniformity of one color pattern. This value is often calculated by means of the ratio $[\Delta uv(x,y)]_{min}/[\Delta uv(x,y)]_{max}$ or by the fraction of points where $\Delta uv(x,y)$ value is below a specified threshold [22]. However, these merit functions present some limitations as a metric if the color pattern has a profile that contains large color deviations. We propose a merit function for color uniformity, which is the RMS (root-mean square) color variation. For example, Δuv_{RMS} function can be computed in function of target distance:

$$\Delta uv(z)_{RMS}=\sqrt{\frac{1}{M}\sum_x\sum_y\Delta uv(x,y,z)^2}\quad , \tag{19}$$

where M is simply the number of sampling points (calculated values of Δuv), which are located at a representative section of the illuminated surface, and are at an equal distance from each other. Depending on the application, Δuv_{RMS} can be computed in function of some other important parameters like packaging density, $\theta_{½}$, number of LEDs, CCT, etc.

3. Example: RGB array

In order to show some features of our analytic procedure, in this section we analyze three popular configurations for RGB assemblies.

3.1 Linear array

We consider a linear RGB array for 3 configurations, R-G-B, G-B-R, y B-R-G (see Fig. 3(a)). The array is configured with 4 LEDs for each color. To calculate $\Delta uv_{RMS}(z)$ we choose a rectangle region of the color pattern (for M=800 sampling points, which are evenly located) defined by $-x_{90}<x<x_{90}$ and $-y_{90}<y<y_{90}$. Limits x_{90} and y_{90} are given by the value of x and y (along a straight line at y=0 or x=0) when illuminance is 10% of the value at the pattern center (x=0,y=0). Extension of the sampling area changes with distance z.

Figures 3(b), (c), and (d) compare the color shift of 3 configurations for Lambertian-type LEDs, with a usual viewing angle $\theta_{½}$=60º of high-brightness LEDs. Figure 4 shows color variation for the 3 configurations of Fig. 3 for typical emitters with a batwing radiation pattern, i.e. n=35, C=0.9, and α=35º.

Figures 3 and 4 are plotted with the following parameters: (1) LEDs emit light with peak wavelengths and half spectral widths (typical parameters of Luxon® emitters): λ_R=625nm and $\Delta\lambda_R$=20nm (red); λ_G=530 nm and $\Delta\lambda_G$=35nm (green); and λ_B=470 nm and $\Delta\lambda_B$=25nm (blue).

#78265 - $15.00 USD Received 19 December 2006; revised 27 February 2007; accepted 28 February 2007

(2) RGB relative irradiances are selected to obtain the chromatic coordinates (x_d=0.313, y_d=0.329) of illuminant D_{65} in the central point of the illuminated region at z=10d. Here d is the LED-to-LED spacing.

Figures 3(d) and 4(b) show that the color distribution of the configuration R-G-B is slightly more uniform for both Lambertian-type LEDs and Batwing-type LEDs, in particular for z>2d. In chromaticity diagrams (Figs. 3(c) y 4(a)), one can see that the locus of color points rotates for each configuration by nearly the same angle. As to be expected, the array with Lambertian-type LEDs produces a more uniform color distribution than with Batwing-type LEDs.

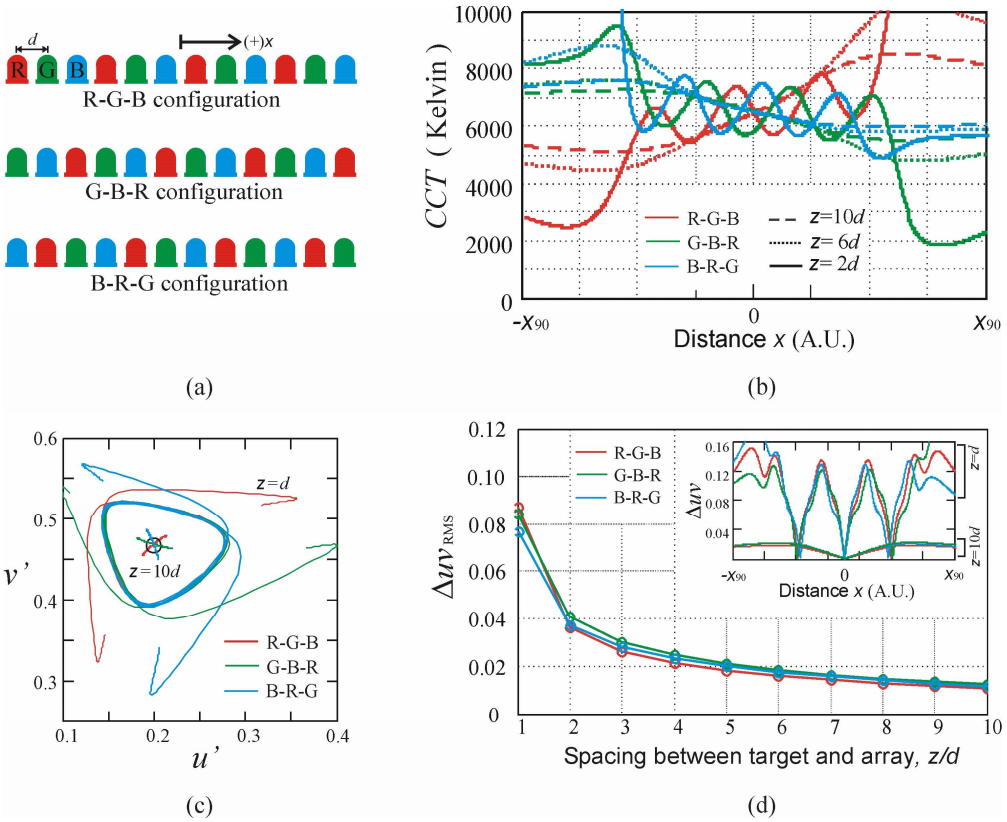

Fig. 3. (a) Schematic of the 3 configurations used for simulating a RGB linear array. Parameter d is the spacing between LEDs. (b-d) Simulations with Lambertian-type LEDs. (b) Spatial distribution of CCT(x,0,z) for z=2d, 6d, and 10d. (c) CIE u'v' 1976 coordinates along the x direction at y=0 for $-x_{90}<x<x_{90}$. (d) The calculated color uniformity $\Delta uv(z)_{RMS}$ in function of the target distance. Inset: color distribution $\Delta uv(x,0,d)$ and $\Delta uv(x,0,10d)$.

3.2 Ring array

One of the most popular arrangements in LED lanterns is the circular ring array. We consider the case of an array with three circular rings (Fig. 5(a)) for 3 RGB configurations. To calculate $\Delta uv_{RMS}(z)$ we choose a circular region of the color pattern (for M=248 sampling points, which are evenly located) defined by $(x^2+y^2)^{1/2}<r_{90}$. Limit r_{90} is the largest radius when illuminance is 10% of the maximum value.

In Figs. 5(b) and (c) we compare the color distribution of 3 configurations for Lambertian-type LEDs, with a narrow viewing angle $\theta_{1/2}$=20º. LEDs are simulated with the peak wavelengths and half spectral widths that we used in Sec. 3.1. We set the color of illuminant D_{65} in the central point of the color distribution in z=3ρ. The radius and the number

#78265 - $15.00 USD Received 19 December 2006; revised 27 February 2007; accepted 28 February 2007

of LEDs of each ring are $\rho_1=\rho$ (12 LEDs), $\rho_2=1.2\rho$ (18 LEDs), and $\rho_3=1.4\rho$ (24 LEDs). Figure 5(a) does not show the number of LEDs (54) used in the simulation.

From Δuv_{RMS}, the color distribution of the — configuration is slightly more uniform as Fig. 5(c) shows. However, it is the opposite situation for CCT (inset in Fig. 5(c)). This behavior becomes evident when we observe the locus orientation of — configuration in Fig. 5(b).

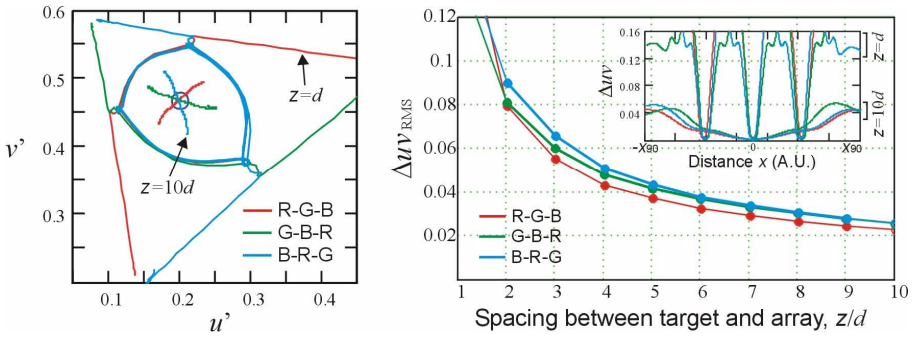

Fig. 4. Simulations with batwing-type LEDs for the arrays analyzed in Fig. 3. (a) CIE $u'v'$ 1976 coordinates along the x direction at y=0 for $-x_{90}<x<x_{90}$. (b) The calculated color uniformity $\Delta uv(z)_{RMS}$ in function of the target distance. Inset: color distribution $\Delta uv(x,0,d)$ and $\Delta uv(x,0,10d)$.

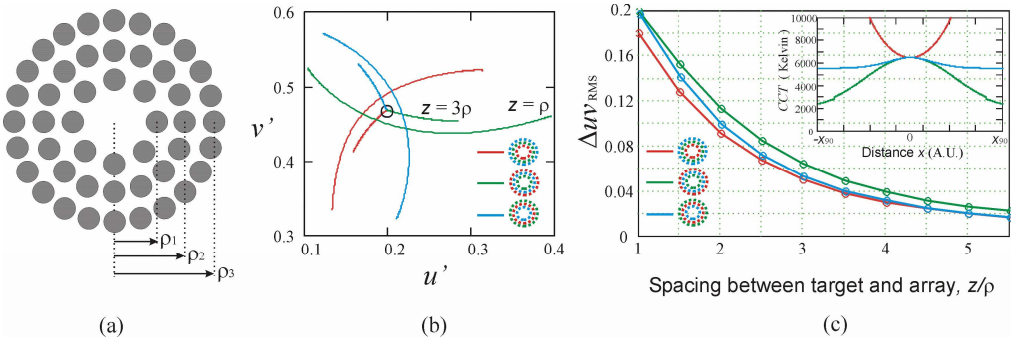

Fig. 5. (a) Circular ring array of LEDs with 3 rings. (b) CIE $u'v'$ 1976 coordinates along the radial direction ($<r_{90}$) for 3 RGB configurations. (c) The calculated color uniformity $\Delta uv(z)_{RMS}$ in function of the target distance. Inset: Spatial distribution of CCT(x,0,z) for z=3ρ.

3.3 Square array

Another typical example is square array. We calculate the color distribution of 3 RGB configurations for an array of 36 LEDs with 12 side emitting LEDs of each color (see Fig. 6(a)). Figures 6(b) and (c) compare the color distribution of the 3 configurations for Luxon® side emitters (see Fig. 2). LEDs are simulated with the peak wavelengths and half spectral widths that we used in Sec. 3.1. Because side emitters have the ability to fill large areas within a short distance, we set the color of illuminant D_{65} in the central point of the color distribution in z=2d. Here d is the LED-to-LED spacing along the x direction, and the spacing between LEDs along the y axis is 3d.

In chromaticity diagram (Fig. 6(b)), again one can see that the locus of color points rotates for each configuration by nearly the same angle. Figure 6(c) shows that the color distribution of the configuration B-R-G is slightly more uniform, mainly at short distances, e.g. z=0.2d.

#78265 - $15.00 USD Received 19 December 2006; revised 27 February 2007; accepted 28 February 2007

The method presented here provides a practical way to perform colorimetric analyses of diverse multicolor LED arrays. We have analyzed some simple configurations in [23], and mathematical representations of the relative irradiance from several configurations of LED arrays are employed in [14,15].

In addition, due to the analytical nature of our theory, it may be useful to choose both the optimal array configuration and the optimal array-diffuser distance for lighting systems with color mixing devices. A lighting system with diffusers is modeled with time consuming numerical software, which is mainly by trial an error. In particular, the dependence of Δuv_{RMS} on either the configuration geometry or the z distance can be used as a tool to choose the starting point parameters to reduce the computation time.

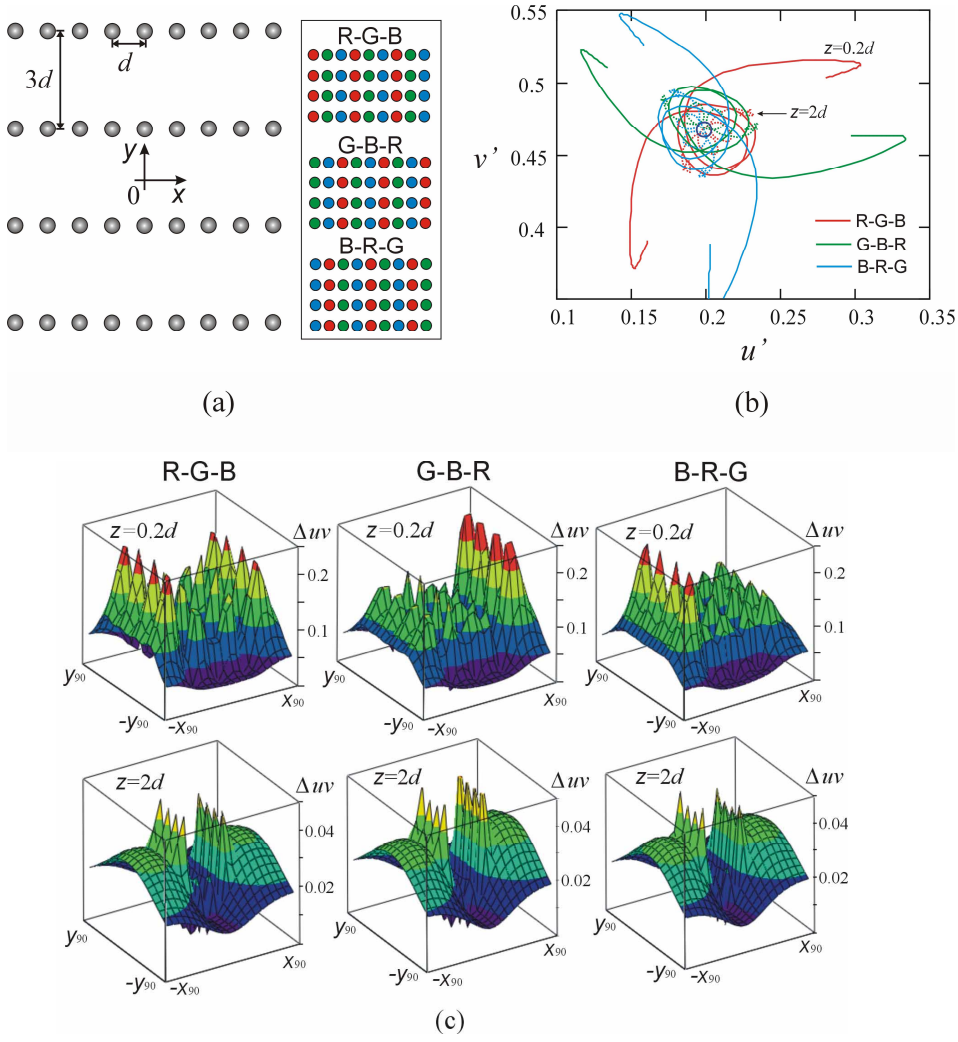

Fig. 6. (a) Rectangular RGB array with 36 side emitting LEDs. (b) CIE $u'v'$ 1976 coordinates along the x direction at y=0 for $-x_{90}<x<x_{90}$.. (c) The calculated color distribution, $\Delta uv(x,y,0.2d)$ and $\Delta uv(x,y,2d)$, on an illuminated surface within an area of $2x_{90} \times 2y_{90}$.

4. Experimental verification

For the purpose of demonstration, we assembled a linear RGB array with R-G-B configuration. The array is assembled with 5 high-power LEDs for each color. The mounted LEDs (LUMILED® catalog number LXHL-ND94 red, LXHL-NM98 green, and LXHL-

#78265 - $15.00 USD Received 19 December 2006; revised 27 February 2007; accepted 28 February 2007

NRR8 royal blue) have a narrow Lambertian-type pattern with a standard viewing angle $\theta_{½}$=5º. We measured the viewing angle for each color, which resulted in θ_R =4.8º, θ_G=6º, and θ_B=5.8º. The measured values for $\theta_{½}$ are the values we used in the simulations. We simulated the spectral distribution, Eq. (4), with the measured peak wavelengths and half spectral widths: λ_R=640nm and $\Delta\lambda_R$=20nm (red); λ_G=530 nm and $\Delta\lambda_G$=35nm (green); and λ_B=460 nm and $\Delta\lambda_B$=20nm (blue).

We assembled the LEDs with an LED-to-LED distance of d=2.5cm over an aluminum plate to dissipate heat. The relative irradiances (at the center of color pattern at z_0=70cm) were $e_{G\text{-}R}$=0.529, $e_{B\text{-}R}$=0.559 (experiment), and $e_{G\text{-}R}$=0.524, $e_{B\text{-}R}$=0.565 (theory) to produce a CCT(0,0,70cm)=6430K with chromatic coordinates (x=0.31,y=0.359). LEDs operated at 145mA (red), 130mA (green), and 200mA (blue). The center point of array was aligned with the optical axis. A fiber optic spectrometer (Ocean Optics USB2000) was positioned in front of the LED panel (see Fig. 7(a)). The color coordinates of the LED array were measured at nine equally spaced points in a horizontal direction through the center of the optical axis, forming a strip $2x_{90}$ long (for experiment x_{90} was measured, and for theory x_{90} was simulated). The theoretical and experimental data are plotted in Figs. 7(c) and 7(d). CIE u'v' coordinates and CCT were measured using OOIIrrad-C (a color measurement software associated with the spectrometer).

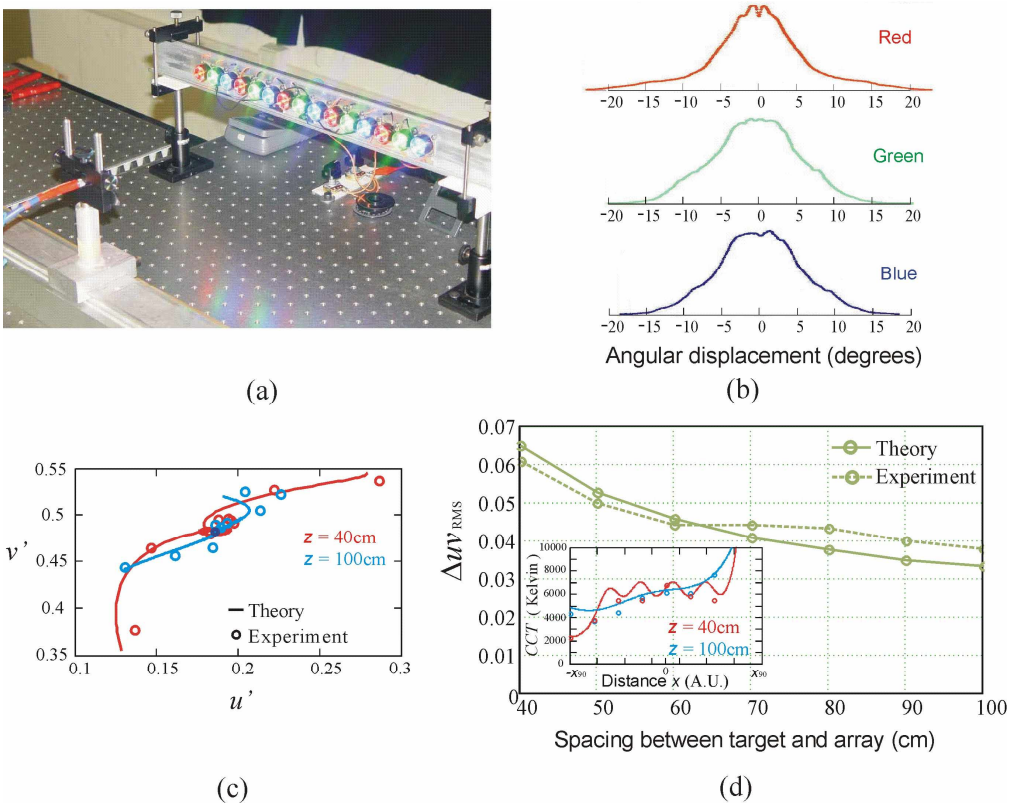

Fig. 7. (a) Experimental setup to measure the color distribution of the light emitted from a linear RGB array. (b) Shows the measured intensity distribution (normalized) of red, green, and blue LEDs. (c) Measured and calculated CIE $u'v'$ 1976 coordinates along the x direction at y=0 for $-x_{90}<x<x_{90}$ (x_{90} is calculated for theory and it is measured for experiment). (d) The color uniformity $\Delta uv(z)_{RMS}$ in function of the target distance. Inset: Spatial distribution of CCT(x,0,z).

The slight disagreement between experimental and modeled data is explained by the fact that the simulated irradiance distribution is not equal to the measured pattern (Fig. 7(b)). Also, spatial and spectral patterns of assembled LEDs are not equal even among LEDs of the same

#78265 - $15.00 USD Received 19 December 2006; revised 27 February 2007; accepted 28 February 2007

type. Nevertheless, the locus of measured points nearly follows that of theory (Fig. 7(c)), and the absolute discrepancy between theory and experiment is near the threshold of visual discrimination ($\leq$0.005) for this region of CIE 1976 diagram [3,4]. In summary, experimental data agreed quite well with theoretical expectations, even though we used ideal parameters for simulations.

5. Conclusion

We have presented a practical all-analytical method for computing the color distribution of the lighting pattern produced by a multicolor LED array. This analytical method can be a practical tool for both a quick estimation (first-order analysis) and as a starting point (to reduce the computation time) for the exact analysis that is performed with commercial optical software packages. This same method can be easily applied to compute angular color distribution by using radiant intensity instead of irradiance [18].

In order to show some features of our analytic procedure, we analyzed three popular configurations for RGB arrays. However, the method can be applied to any other multicolor array configuration, which is only limited by the imagination. Additionally, color distribution can be computed in function of some other important parameters like viewing angle ($\theta_{½}$), the number of LEDs, and the CCT.

Other possible applications of this analytic technique include computation of: color rendering index distribution; and angular color distribution of multichip LEDs, which requires knowing the intensity distribution of each single chip [22].

Acknowledgments

This research was supported by CONACYT (Consejo Nacional de Ciencia y Tecnologia) grant J48199-F. We thank Maureen Sophia Harkins, cetet@uaz.edu.mx, for proofreading this paper.

#78265 - $15.00 USD Received 19 December 2006; revised 27 February 2007; accepted 28 February 2007